ACS APPLIED MATERIALS & INTERFACES

RESEARCH ARTICLE

www.acsami.org

Ultraviolet Random Lasing Action from Highly Disordered *n*-AlN/*p*-GaN Heterojunction

H. Y. Yang,[†,*] S. F. Yu,[*,‡] J. I. Wong,[†] Z. H. Cen,[§] H. K. Liang,[§] and T.P. Chen[§]

[†]Pillar of Engineering Product Development, Singapore University of Technology and Design, Singapore 279623

[‡]Department of Applied Physics, The Hong Kong Polytechnic University, Hung Hum, Kowloon, Hong Kong

[§]School of Electrical & Electronic Engineering, Nanyang Technological University, Singapore

ABSTRACT: Room-temperature random lasing is achieved from an *n*-AlN/*p*-GaN heterojunction. The highly disordered *n*-AlN layer, which was deposited on *p*-GaN:Mg layer via radio frequency magnetron sputtering, acts as a scattering medium to sustain coherent optical feedback. The *p*-GaN:Mg layer grown on sapphire provides optical amplification to the scattered light propagating along the heterojunction. Hence, lasing peaks of line width less than 0.4 nm are emerged from the emission spectra at round 370 nm for the heterojunction under forward bias larger than 5.1 V. Lasing characteristics of the heterojunction are in agreement with the behavior of random lasers.

KEYWORDS: highly disordered AlN thin films, ultraviolet random lasing, laser diode

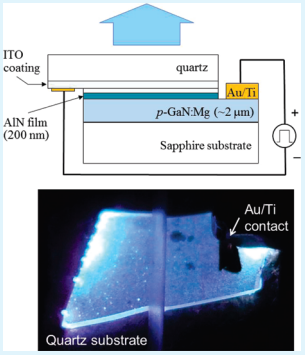

INTRODUCTION

Extensive investigations on the optical properties of highly disordered random systems have revealed that the presence of multiple optical scattering and light amplification can sustain random lasing action.[1] Under external optical excitation, the formation of localized lights with UV and visible wavelengths has been reported in either highly disordered or nanostructured semiconductor materials such as ZnO, GaN, GaAs, and SnO_2.[2−5] Currently, battery-driven random laser diodes have also been fabricated by using cluster of ZnO nanocrystals, highly disordered ZnO thin films, and vertically aligned ZnO nanorods as the optical cavities to provide multiple optical scattering and light amplification simultaneously.[6−11] However, there is a drawback to using ZnO as the random cavities—stable and high-conductivity *p*-type ZnO-based materials are still difficult to achieve.[12] As a result, the ZnO based random laser diodes may suffer from low electrical-to-optical conversion efficiency and the use of ZnO will limit the future development of electrical pumped random lasers. However, it is highly desired to use electrical pumped random lasers as board-band low-coherence sources to suppress coherent noise in optical systems[13] such as in CD and DVD players, and to improve depth-resolved images of optical coherence tomography[14] and photorefractive holography.[15]

Nowadays, the realization of random laser diodes is still restricted to the use of ZnO as the optical cavities. This is because (1) highly scattered random medium can be easily obtained from ZnO to support coherent optical feedback and (2) ZnO can provide extremely high excitonic gain at room temperature. Hence, ZnO remains to be the first choice for the realization of random laser diodes. In this paper, we proposed to use *p*-GaN as the optical gain and highly disordered *n*-AlN layer as the optical scattering medium for the realization of electrical pump random lasers. The choice of *n*-AlN/*p*-GaN heterojunction will favor radiative recombination of external injection of carriers inside the *p*-GaN. In addition, the propagation of amplified spontaneous emission (ASE) inside the *p*-GaN will experience distributed multiple optical scattering from the AlN layer to sustain coherent optical feedback. Hence, this implies that the realization of random laser diodes can be less dependent on the choice of optical materials as the optical gain and highly scattered medium can be spatially separated. This design will allow the further development of reliable and high-performance electrical pumped random lasers by avoiding use of ZnO-based random cavities.

RESULTS AND DISCUSSION

Figure 1 shows the schematic of a *p*−*n* heterojunction diode. A ∼4 × 6 mm^2 *p*-GaN (∼2 μm thick)/sapphire substrate (from Semiconductor wafer Inc., Taiwan) was chosen to be the supporting substrate and hole-injection layer of the diode. About 200 nm thick of highly disordered AlN was deposited onto the surface of the *p*-GaN/sapphire substrate by radio frequency magnetron sputtering to form a heterojunction.[16,17] About 100 nm thick of indium tin oxide (ITO) was coated onto the AlN surface as a cathode ohmic contact. Quartz substrate deposited with ITO, which is in physical contact with the ITO coated on the AlN surface, was use to inject electrons to the heterojunction. Au (100 nm)/Ti (20 nm) metal layer was deposited onto the *p*-GaN layer as an anode ohmic contact for the injection of holes.

Images a and b in Figure 2 show the scanning electron microscopy (SEM) images of the surface of the uncoated

Received: February 23, 2011
Accepted: April 11, 2011
Published: April 11, 2011

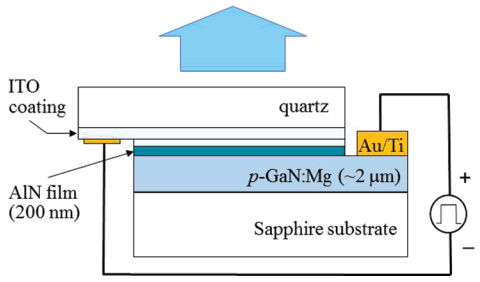

Figure 1. Schematic diagram of the *n*-AlN/*p*-GaN:Mg heterojunction.

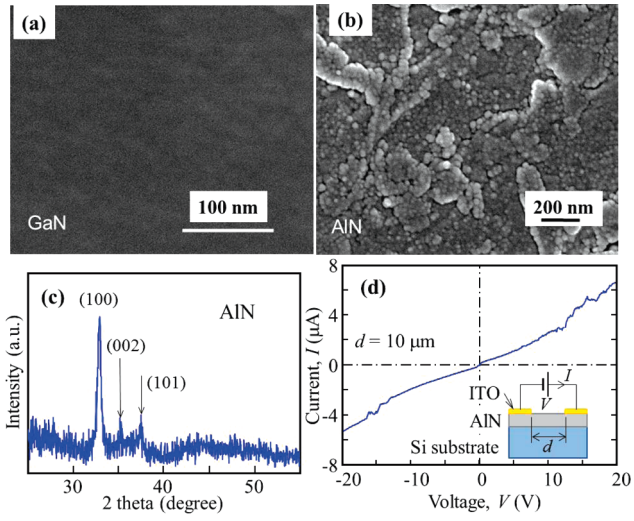

Figure 2. (a) SEM image of GaN surface, (b) SEM image of InN surface, (c) XRD pattern of AlN thin film on *p*-GaN/sapphire substrate, and (d) current−voltage (*I*−*V*) characteristic of the ITO/AlN ohmic contacts.

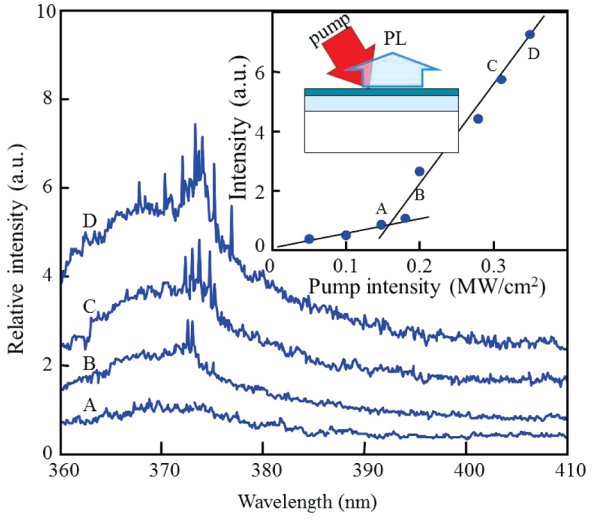

Figure 3. PL spectra of the *n*-AlN/*p*-GaN:Mg heterojunction. The insert shows the light−light curve of the *n*-AlN/*p*-GaN:Mg heterojunction.

p-GaN/sapphire substrate and the AlN layer deposited onto the *p*-GaN/sapphire substrate. It is noted that the *p*-GaN/sapphire substrate has a very smooth surface but the deposited AlN layer's surface is very rough. Grains from few tens to thousands of nm are observed from the surface of the AlN layer. Figure 2c gives the X-ray diffraction (XRD) pattern of the as-grown AlN thin film deposited on the *p*-GaN/sapphire. The XRD peaks at $2\theta = 33.1$, 35.9, and 37.8° can be assigned to the (100), (002), and (101) reflections respectively, of a wurzite hexagonal-phase with lattice parameters of $a = 3.1114$ Å and $c = 4.9792$ Å.[18] The peak of highest intensity at $2\theta = 33.1°$ indicated that the sample is mainly formed by crystallites oriented at the *a*-axis direction. Current−voltage (*I*−*V*) curve of the ITO contacts (separated by a distance $d = 10\ \mu$m) deposited on a 200 nm thick AlN layer was also measured, see Figure 2d. It is noted that the relationship between *I* and *V* is roughly linear for the absolute *V* less than 20 V.

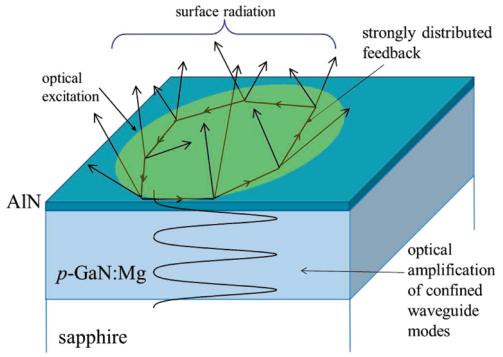

Figure 4. Schematic diagram explains the light confinement and scattering processes inside the *n*-AlN/*p*-GaN:Mg heterojunction.

Figure 3 shows the photoluminance (PL) spectra of the *n*-AlN/*p*-GaN:Mg heterojunction without ITO contact on the *n*-AlN layer. The corresponding light−light curve is also plotted in the insert of the figure. Single broad ASE spectra with peak and full-width at half-maximum (fwhm) of ~370 and ~14 nm respectively are observed from the PL spectra. These ASE spectra represent the direct bandgap radiative recombination from the GaN layer. A kink (i.e., pump threshold[1]) is observed from the light−light curve at a pumped intensity equal to ~0.5 MW/cm^2. Sharp peaks at wavelength around 374 nm with line width less than 0.4 nm emerged from the emission spectra from the pump intensity larger than the pumped threshold. Furthermore, the number of sharp peaks increases with the increase of pumped intensity. Hence, it is believed that the sample exhibits random lasing characteristics under external optical excitation. This is because GaN layer provides optical gain and AlN layer supplies strong multiple optical scattering of the heterojunction to sustain random lasing action. Figure 4 explains the optical confinement characteristics and lasing mechanism of the heterojunction. It is noted that the refractive indices (ordinary ray) of sapphire, AlN, and GaN are roughly equal to 1.79, 2.21, and 2.64, respectively, at ~370 nm.[19] Hence, the heterojunction structure forms an optical waveguide to confine light within the GaN layer. As the GaN layer has higher refractive index than that of the AlN and sapphire, light can be trapped and propagated inside the GaN layer via total internal reflection. Furthermore, the light experiences distributed multiple optical scattering inside the AlN layer so that it is possible to obtain closed-loop paths for light within the region under optical excitation. In fact, the configuration of the *n*-AlN/*p*-GaN:Mg heterojunction is similar to that of a surface-emitting distributed feedback (DFB) laser. This is because the AlN layer works like a grating layer of the DFB laser.

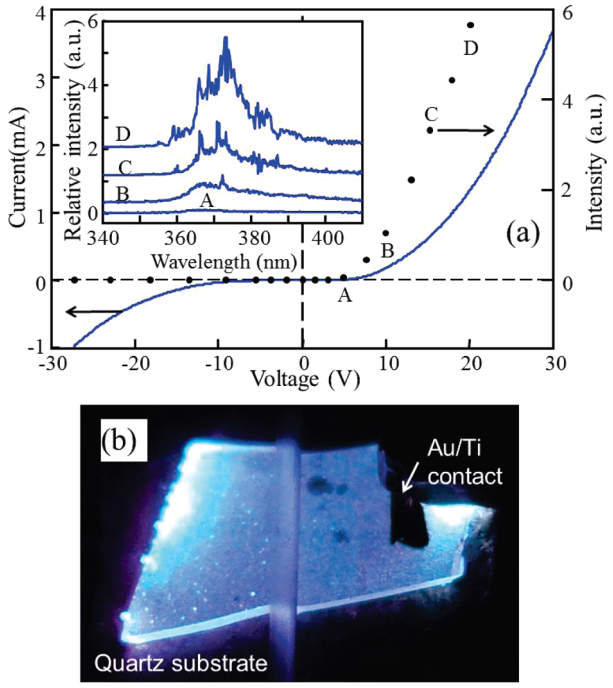

Figure 5. (a) Current−voltage and intensity−voltage curves of the *n*-AlN/*p*-GaN:Mg heterojunction. The insert shows the EL spectra of the *n*-AlN/*p*-GaN:Mg heterojunction under forward bias. (b) Photo taken from the surface of the *n*-AlN/*p*-GaN:Mg heterojunction under forward bias at about 15 V.

Hence, lasing light (sharp peaks) can be observed from the surface of the heterojunction. In addition, lasing light has multiple directions—it can emit all over the space from the surface of the AlN layer.

Figure 5a compares the $I-V$ and light-voltage ($L-V$) curves of the *n*-AlN/*p*-GaN heterojunction diode under forward and reverse bias. It is observed that the $I-V$ curve exhibits a rectifying behavior and with a turn-on voltage of ~5.1 V. However, the turn-on voltage is larger than that the bandgap of GaN due to the wide bandgap of the AlN layer. It may also be related to the high ohmic resistance from the ITO contact on the AlN layer. On the other hand, for the reverse bias larger than 10 V, large leakage current is observed for the $I-V$ curve. The insert of figure 5a plots the corresponding electroluminance (EL) spectra of the heterojunction under forward bias. A single broad ASE spectrum with peak and fwhm of ~370 and ~7 nm respectively is observed from all the EL spectra. Furthermore, sharp peaks of line width less than 0.4 nm are emerged from the EL spectrum for bias voltage above the turn-on voltage. In addition, the number of sharp peaks increases with the increase of bias voltage. The above observations have indicated that the heterojunction demonstrates lasing characteristics under electrical excitation and the lasing characteristics are similar to that under optical excitation. Figure 5b shows a photo of the heterojuction taken at forward bias of about 15 V. Blue-violet emission is clearly observed from the entire sample. This is because the waveguide effect of the heterojunction allows the propagation of ASE along the GaN layer. At the region under the quartz substrate especially near the edges of the sample, blue emission intensity is very high. This is due to the optical scattering of ASE, which is obtained from the GaN:Mg layer under the external injection of carriers, via the multiple optical scattering of the AlN layer. In addition, light

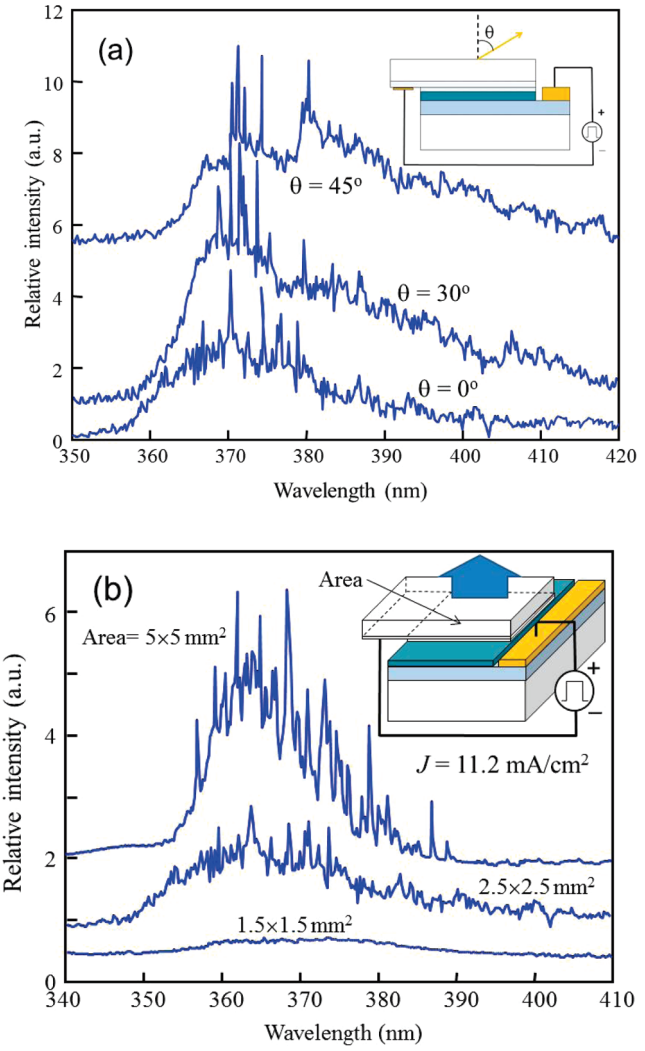

Figure 6. EL spectra observed from (a) different angles from the surface, and (b) different ITO's contact area of the heterojunction.

emission from the edge of the sample is favored because of the optical confinement structure of the heterojunction diode.

In order to verify that the sample exhibits random lasing action under electrical excitation, we have examined the emission spectra from the heterojunction at different angles of observation as well as with different excitation areas. Figure 6a shows the EL spectra observed from the surface of the heterojunction at different directions. The heterojunction was biased at 15 V throughout the experiment. It is noted that the emission spectra are different at different observed angles. This is because different laser cavities formed by multiple scattering can have different output directions so that the lasing spectra observed at different angles are different. Figure 6b shows the EL spectra of the heterojunction with different area of ITO contact deposited onto the AlN layer. The bias current density, J, was maintained at ~11.2 mA/cm^2 for all the samples. It is observed that before the critical contact area (i.e., 1.5 × 1.5 mm^2) is reached, no shape peak is excited. However, when the ITO's area has exceeded the threshold, sharp lasing peaks with line width less than 0.4 nm emerge from the spectrum. The number of sharp peaks increases with the increase of ITO's area. This is because in a large excitation area, more closed-loop paths for light can be formed.

dx.doi.org/10.1021/am2002372 |*ACS Appl. Mater. Interfaces* 2011, 3, 1726–1730

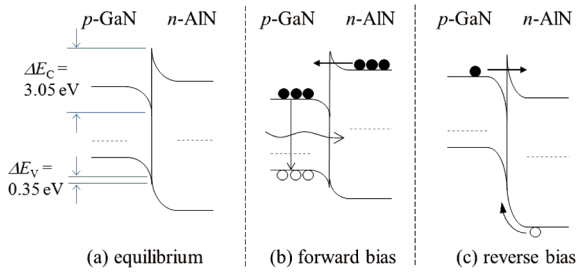

Figure 7. Band diagram of the *n*-AlN/*p*-GaN:Mg heterojunction at (a) equilibrium, (b) forward bias, and (c) reverse bias.

As a result, random laser action could occur in more cavities formed by recurrent scattering. However, if the ITO's area is reduced below a critical size, lasing oscillation stopped. This is because if the closed-loop paths are too short, the amplification along the loops is not high enough to achieve lasing.[1]

Figure 7 shows the energy-band diagram of the *n*-AlN/*p*-GaN heterojunction under the conditions of equilibrium, forward and reverse bias. We have assumed that the AlN layer is in good contact with the GaN surface so that their vacuum levels can be roughly continued across the heterojunction. If the electron affinity energies of AlN and GaN are chosen to be ~0.25 and ~3.3 eV, respectively, the bandgap energy of AlN is set to ~6.0 eV and that of GaN is chosen to ~3.3 eV.[20,21] Then, it can be shown that the conduction band offset, ΔE_C, and valence band offset, ΔE_V, of the AlN/GaN heterojunction are roughly equal to 3.05 and 0.35 eV respectively. The Fermi level of *p*-GaN can be estimated to be around 0.8 to 1.0 eV above the valence band due to the high carrier concentration of *p*-GaN:Mg. For AlN layer, the Fermi level can be varied between 2.8 and 3.0 eV below the conduction band as the corresponding carrier concentration is low. For the heterojunction under forward bias, electron from the *n*-AlN can be tunneled through the thin barrier to the *p*-GaN. However, holes from *p*-GaN are blocked by the barrier of AlN. Hence, electrons and holes are favored to be recombined radiatively inside the *p*-GaN layer, see figure 7b. This is the reason why we observed emission spectra with peak wavelength at ~370 nm (i.e., bandgap energy of GaN) and blue-violet light is generated mostly inside the GaN layer. Figure 7c shows the heterojunction under reverse bias condition. At high reverse condition, electrons at the *p*-GaN layer can be tunneled through the barrier at the condition band of the *n*-AlN so that high leakage current can be observed. Hence, we have explained the observed optical and electrical properties of the *n*-AlN/*p*-GaN heterojunction.

SUMMARY

In summary, we have demonstrated random lasing action from an *n*-AlN/*p*-GaN heterojunction under electrical excitation at room temperature. Optical feedback mechanism of the heterojunction is similar to that of a surface-emitting (i.e., second order grating) DFB lasers except the uniform grating is replaced by a highly disordered AlN layer. This is because optical modes supported inside the GaN layer can be scattered into multiple directions by the AlN layer. Hence, closed-loop path for light is achieved and coherent random lasing is observed from the heterojunction. The variation of lasing patterns over different observation angles and the dependence of lasing threshold (i.e., emerge of sharp peaks) on the excitation area have verified that the lasing mechanism is due to random lasing action. Furthermore, it can be shown that the profile of lasing spectra can be maintained unchanged for few hours. Hence, the long-term stability of the laser diodes can be compatible or better than that of the existing random laser diodes. Other advantage of using AlN layer is that it can confine the injection carriers into the *p*-GaN layer so that strong ASE can be obtained from the heterojunction under forward bias. The observation of broad emission peak of the spectra at ~370 nm (i.e., bandgap energy of GaN) has verified that strong ASE is attributed to the direct bandgap radiative recombination inside the *p*-GaN layer. Furthermore, when compared to the performance of the existing random laser diodes,[6−11] the proposed *n*-AlN/*p*-GaN heterojunction (1) has better electrical-to-optical conversion efficiency due to the use of *p*-GaN as the gain region, (2) can be easily optimized its performance due to the spatial separation of optical gain and scattering region, and (3) has potential to be commercialized due to the matured GaN technology. Optical characteristics of the proposed *n*-AlN/*p*-GaN heterojunction, however, should be similar to the existing random laser diodes—light is emitted in multiple directions.

FABRICATION AND MEASUREMENT METHODS

Fabrication. A 200 nm thick of AlN film was first deposited on a cleaned *p*-type GaN:Mg (~2 μm)/sapphire substrate (purchased from Semiconductor Wafer Inc., Taiwan) by radio frequency magnetron sputtering technique. The sputter target was a pure Al (99.99%) placed at a distance 8 cm and at an angle 30° to the surface of the *p*-GaN:Mg/sapphire substrate. The AlN layer was grown under the flow of pure N_2 and Ar gases at a flow rate of 30 and 15 SCCM, respectively so that the chamber pressure was maintained between 6×10^{-3} and 10×10^{-3} mbar. The sputtering growth was done for 1 h, at a sputtering power of 300 W with substrate temperature at 25 °C. Bilayer Ti(20 nm)/Au-(100 nm) electrode was deposited on the *p*-GaN:Mg by thermal evaporation as the *p*-ohmic contact. A 100 nm thick of ITO was deposited on the AlN layer by sputtering as the *n*-ohmic contact at room temperature.

EL and PL Measurement. The heterojunction diode was driven by a rectangle pulse voltage source with repetition rate and pulse width of 7.5 Hz and 80 ms, respectively. Light was collected from the uncoated side of the quartz substrate by an objective lens. PL spectra of the samples at room temperature were studied under optical excitation by a Nd:YAG (355 nm: YAG: yttrium aluminum garnet) laser operating in pulsed mode (6 ns, 10 Hz). An optical beam of diameter ~10 mm was excited at an angle to the surface of the AlN layer. Emission was collected in the direction perpendicular to the surface of the AlN by an objective lens.

AUTHOR INFORMATION

Corresponding Author

*E-mail: yanghuiying@sutd.edu.sg (H.Y.Y.); sfyu21@hotmail.com (S.F.Y.).

ACKNOWLEDGMENT

This work was supported by HK PolyU Grant (1-ZV6X), SUTD Grant (SRG EPD 2010-003), and Loreal Singapore for Women in Science National fellowship.

REFERENCES

(1) Cao, H. *Waves Random Media* **2003**, *13*, R1–R39.
(2) Cao, H.; Zhao, Y. G.; Ho, S. T.; Seelig, E. W.; Wang, Q. H.; Chang, R. P. H. *Phys. Rev. Lett.* **1999**, *82*, 2278–2281.

(3) Sakai, M.; Inose, Y.; Ema, K.; Ohtsuki, T.; Sekiguchi, H.; Kikuchi, A.; Kishino, K. *Appl. Phys. Lett.* **2010**, *97*, 151109.
(4) Noginov, M. A.; Zhu, G.; Fowlkes, I.; Bahoura, M. *Laser Phys. Lett.* **2004**, *1*, 291–293.
(5) Yang, H. Y.; Yu, S. F.; Lau, S. P.; Tsang, S. H.; Xing, G. H.; Wu, T. *Appl. Phys. Lett.* **2009**, *94*, 241121.
(6) Leong, E. S. P.; Yu, S. F. *Adv. Mater.* **2006**, *18*, 1685–1688.
(7) Leong, E. S. P.; Yu, S. F.; Lau, S. P. *Appl. Phys. Lett.* **2006**, *89*, 221109.
(8) Chu, S.; Olmedo, M.; Yang, Z.; Kong, J. Y.; Liu, J. L. *Appl. Phys. Lett.* **2008**, *93*, 181106.
(9) Ma, X. Y.; Chen, P. L.; Li, D. S.; Zhang, Y. Y.; Yang, D. R. *Appl. Phys. Lett.* **2007**, *91*, 251109.
(10) Zhu, H.; Shan, C. X.; Yao, B.; Li, B. H.; Zhang, J. Y.; Zhang, Z. Z.; Zhao, D. X.; Shen, D. Z.; Fan, X. W.; Lu, Y. M.; Tang, Z. K. *Adv. Mater.* **2009**, *21*, 1613–1617.
(11) Ma, X. Y.; Pan, J. W.; Chen, P. L.; Li, D. S.; Zhang, H.; Yang, Y.; Yang, D. R. *Opt. Express* **2009**, *17*, 14426–14433.
(12) Avrutin, V.; Silversmith, D. J.; Morkoc, H. *Proc. IEEE.* **2010**, *98*, 1269–1280.
(13) Pawluczyk, R. *Appl. Opt.* **1989**, *28*, 3871–3881.
(14) Gu, Y.; Ansari, Z.; Dunsby, C.; Parsons-Karavassilis, D.; Siegel, J.; Itoh, M.; French, P. M. W.; Nolte, D. D.; Headley, W.; Melloch, M. R. *J. Mod. Opt.* **2002**, *49*, 877–887.
(15) Brown, W. J.; Pyhtila, J. W.; Terry, N. G.; Chalut, K. J.; D'Amico, T. A.; Sporn, T. A.; Obando, J. V.; Wax, A. *IEEE J. Select. Topics Quantum Electron.* **2008**, *14*, 88–97.
(16) Yong, Y. J.; Lee, J. Y.; Kim, H. S.; Lee, J. Y. *Appl. Phys. Lett.* **1997**, *71*, 1489–1591.
(17) Pelegrini, M. V.; Pereyra, I. *Phys. Status Solidi C* **2010**, *7*, 840–843.
(18) Garcia-Mendez, M.; Morales-Rodriguez, S.; Galvan, D. H.; Machorro, R. *Int. J. Modern Phys. B* **2009**, *23*, 2233–2251.
(19) http://refractiveindex.info/
(20) Choi, J. W.; Puthenkovilakam, R.; Changa, J. P. *Appl. Phys. Lett.* **2005**, *86*, 192101.
(21) Grabowski, S. P.; Schneider, M.; Nienhaus, H.; Monch, W.; Dimitrov, R.; Ambacher, O.; Stutzmann, M. *Appl. Phys. Lett.* **2001**, *78*, 2503–2505.